

Self-steepening of ultrashort optical pulses without self-phase-modulation

Jeffrey Moses,¹ Boris A. Malomed,² and Frank W. Wise¹

¹*Department of Applied and Engineering Physics, Cornell University, Ithaca, New York 14853, USA*

²*Department of Interdisciplinary Studies, Faculty of Engineering, Tel Aviv University, Tel Aviv 69978, Israel*

(Received 23 January 2007; published 28 August 2007)

We report the experimental manifestation in optical physics of wave propagation involving self-steepening without concomitant self-phase-modulation. The conditions are realized through the interplay of quadratic and cubic nonlinearities in a frequency-doubling crystal. The experiment constitutes the physical realization of the Chen-Lee-Liu equation, a derivative nonlinear Schrödinger equation that governs pulse propagation.

DOI: [10.1103/PhysRevA.76.021802](https://doi.org/10.1103/PhysRevA.76.021802)

PACS number(s): 42.65.Sf, 05.45.-a, 42.25.Bs, 42.65.Re

The self-steepening of optical pulses has received much attention since the invention of the femtosecond laser. Its source, in mathematical terms, is the first nonlinear correction to the nonlinear Schrödinger equation (NLSE) for light pulses temporally narrow enough to violate the slowly-varying-envelope approximation [1]. Because of this, self-steepening has been studied only in conjunction with self-phase-modulation (SPM): together, the two nonlinear terms account for the asymmetric spectral and temporal shaping of ultrashort pulses [2].

Outside the realm of nonlinear optics, propagation equations in which self-steepening is the sole nonlinear effect, appearing without SPM, received early attention for their mathematical properties. Like the NLSE, the Kaup-Newell equation (KNE) [3]

$$\frac{\partial a}{\partial \xi} + i \frac{\partial^2 a}{\partial s^2} + \kappa \frac{\partial}{\partial s} (|a|^2 a) = 0 \quad (1)$$

and the Chen-Lee-Liu equation (CLLE) [4]

$$\frac{\partial a}{\partial \xi} + i \frac{\partial^2 a}{\partial s^2} + \kappa |a|^2 \frac{\partial a}{\partial s} = 0, \quad (2)$$

which feature self-steepening without SPM, are integrable. The solvability of the NLSE coupled with its successful modeling of physical systems in many different contexts make it a very special model. By contrast, isolated self-steepening is rarely encountered in nature: manifestations of the KNE and CLL are few. The KNE is only known to model Alfvén waves in magnetized plasmas [5]; the CLL has heretofore not been recognized to describe any physical system.

We show here that the CLL accurately models conditions readily met in a quadratic nonlinear crystal. The equation serves as a model for a mix of cubic and quadratic nonlinearities, with the quadratic terms treated in the cascading limit, corresponding to second-harmonic generation (SHG) with a large wave-vector mismatch. We find conditions under which the effective Kerr-like nonlinearity generated by the cascading cancels with the real cubic term, thus leaving self-steepening in isolation. We experimentally and numerically demonstrate the basic evolution of the CLL and observe an interesting optical phenomenon: self-steepening without simultaneous nonlinear phase modulation results in the tilting of the temporal profile of a pulse and

shock formation, but with little change to the power spectrum. With these observations, one may add the CLL to the short list of nonlinear propagation equations that, like the NLSE, are solvable and may be consistently derived from Maxwell's equations.

The cascaded-quadratic ($\chi^{(2)}:\chi^{(2)}$) nonlinearity makes it possible to impress Kerr-like nonlinear phase shifts of controllable sign and magnitude on pulses [6]. It has been exploited to mimic the propagation of ultrashort pulses under $\chi^{(3)}$, using a quadratic medium [7]. The propagation obeys an effective NLSE with features usually inaccessible from $\chi^{(3)}$, such as a negative (self-defocusing) sign of the Kerr term [8], and Raman- [9] or self-steepening-like [10] terms of controllable sign and magnitude.

We consider the combined action of quadratic and cubic nonlinearities in a phase-mismatched SHG process. The coupled propagation equations for fundamental field (FF) and second-harmonic field (SHF),

$$i \frac{\partial a_1}{\partial \xi} - \frac{\alpha_1}{2} \frac{\partial^2 a_1}{\partial s^2} + \left(1 + i\sigma \frac{\partial}{\partial s}\right) [a_1^* a_2 e^{-i\beta' \xi} + \kappa (|a_1|^2 + \nu |a_2|^2) a_1] = 0,$$

$$i \frac{\partial a_2}{\partial \xi} - i \frac{\partial a_2}{\partial s} - \frac{\alpha_2}{2} \frac{\partial^2 a_2}{\partial s^2} + \left(1 + i \frac{\sigma}{2} \frac{\partial}{\partial s}\right) [a_1^2 e^{i\beta' \xi} + \kappa (|a_2|^2 + \nu |a_1|^2) a_2] = 0, \quad (3)$$

may be reduced to an approximate equation for the FF in the limit of large wave-vector mismatch, leaving only the leading-order nonlinear terms that arise from both quadratic and cubic susceptibilities [10]:

$$\frac{\partial a}{\partial \xi} + i \frac{\partial^2 a}{\partial s^2} - i\alpha |a|^2 a + \beta |a|^2 \frac{\partial a}{\partial s} + \lambda a^2 \frac{\partial a^*}{\partial s} = 0. \quad (4)$$

Here, $s = t/\tau_0 - z/v_{g,1}\tau_0$, $\xi = z(1/v_{g,1} - 1/v_{g,2})/\tau_0$, τ_0 is an arbitrary temporal scale, whereas a_i , $v_{g,i}$ and α_i are amplitudes, group velocities, and the normalized group-velocity dispersion (GVD), respectively, for the FF and SHF. Further, σ is the inverse normalized FF frequency, β' the normalized wave-vector mismatch, κ the normalized cubic nonlinear coefficient, and ν the ratio of cross-phase-modulation to SPM.

In Eq. (4), α , β , and λ are derived from the mix of $\chi^{(2)}$ and $\chi^{(3)}$ effects, and are explicitly defined in Ref. [10].

Equation (4) is a generalized derivative NLSE. For particular choices of coefficients, it is integrable [3,11]. For example, with $\alpha=a$, $\beta=2b$, and $\lambda=b$, it is the cubic NLSE modified to describe the propagation of few-cycle pulses [1]. When $\alpha=0$, it is known as the type-II derivative NLSE. In this case, with $\beta=2$ and $\lambda=1$ it is the KNE, Eq. (1), and with $\beta=1$ and $\lambda=0$ it reduces to the CLLE, Eq. (2).

The sign and size of quadratic components in α , β , and λ are controllable through the wave-vector mismatch ($\Delta k=2k_1-k_2$), while the cubic parts are fixed and proportional to the nonlinear index of refraction, n_2 . Although these coefficients share dependences on material and experimental parameters, for a given material one may achieve reasonable control of their relative values. In particular, Ref. [10] shows that α and λ vanish in unison when the contributions of $\chi^{(2)}$ and $\chi^{(3)}$ to the total effective nonlinear index of refraction, $(n_2)_{\text{tot}}(\Delta k)=n_2+(n_2)_{\text{eff}}^{(\chi^{(2)})}(\Delta k)$, cancel. Since the cubic nonlinear phase shift is usually positive, one may choose Δk so as to make $(n_2)_{\text{eff}}^{(\chi^{(2)})}$ negative and equal in magnitude to n_2 , thus reducing Eq. (4) to the CLLE,

$$\frac{\partial A}{\partial z} + i\frac{\beta_2}{2}\frac{\partial^2 A}{\partial \tau^2} - \left[\frac{\gamma}{\Gamma^2} \left(2\delta + \frac{\Gamma^2}{\omega_0} \right) \right] |A|^2 \frac{\partial A}{\partial \tau} = 0, \quad (5)$$

which occurs when $\Delta k=-\Gamma^2/\gamma \equiv \Delta k_{\text{ZSPM}}$. Here, A is the complex FF pulse envelope, Γ is proportional to $\chi^{(2)}$, and $\gamma=n_0 n_2 \omega_0/2\pi$. Parameters δ and β_2 are the group velocity mismatch (GVM) between the FF and SHF ($\delta=1/v_{g,1}-1/v_{g,2}$) and the GVD coefficient at the FF, respectively. The absence of SPM in Eq. (5) is the result of the balance between $\chi^{(2)}$ and $\chi^{(3)}$ nonlinearities in Eqs. (3): $\chi^{(2)}$ - and $\chi^{(3)}$ -generated nonlinear phase shifts exactly cancel after each cycle of the energy conversion between the FF and SHF. However, the intensity-dependent temporal shift of the energy distribution in the pulse, resulting from the difference in EF and SHF group velocities, does not cancel, making self-steepening the dominant nonlinear effect. In this Rapid Communication, we report conditions found in common bulk quadratic media that yield $\Delta k=\Delta k_{\text{ZSPM}}$, and thereby an experimental implementation of the CLLE.

Numerical simulations of the CLLE, Eq. (5), correctly reproduce the picture revealed by simulations of the full system of Eqs. (3). For example, a clear match between solutions of the full system (solid lines) and CLLE (dotted lines) for zero GVD is shown in Fig. 1. These simulations show the effect of the isolated self-steepening term, which may be interpreted as an intensity-dependent group velocity that transfers energy from the peak of the pulse to its side, tilting the pulse and eventually forming a shock, Fig. 1(a). While there is negligible temporal phase modulation [see Fig. 1(b)], new small-amplitude spectral components emerge symmetrically in the power spectrum [Fig. 1(c)]. These new components, together with the change in spectral phase [Fig. 1(d)], result in the steepening of the temporal profile. In sharp contrast to the common case where self-steepening and SPM act

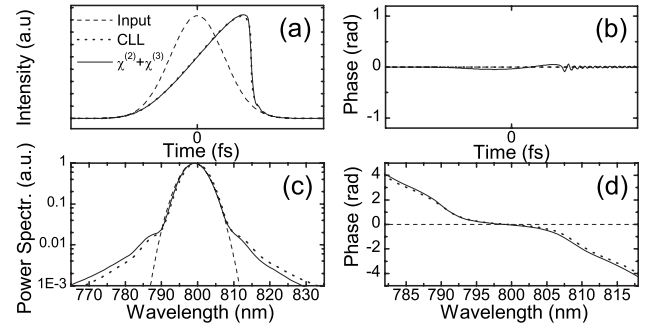


FIG. 1. Isolated self-steepening: the simulated propagation of coupled FF and SHF, as obtained from Eqs. (3) (solid lines) and from the corresponding CLLE, Eq. (5) (dotted lines). Initial conditions (dashed lines) correspond to a FF Gaussian pulse at 800 nm, with a temporal width of 120 fs and intensity of 200 GW/cm². Propagation parameters correspond to a 6-cm-long BBO crystal. In Eqs. (3), Δk is set so as to cancel the $\chi^{(2)}$ and $\chi^{(3)}$ nonlinear phase shifts (see text), and the GVD is artificially set to zero. (a) The FF temporal profile; (b) temporal phase; (c) power spectrum; (d) spectral phase.

together [2], strong steepening of the pulse edge occurs here without a spectral shift and/or generation of conspicuous new spectral components. The inclusion of GVD disrupts the formation of the shock front, but the steepening is still observed if it is initially a stronger effect. In this case, the results of simulations of Eqs. (3) and (5) still agree closely. The degree to which a steepened edge forms depends on the initial pulse width and intensity and the ratio of the GVD and self-steepening coefficients: a maximum steepening is reached, after which the pulse generally decays.

We have observed the predicted pulse steepening directly in experiments, using the common nonlinear crystal β -barium metaborate (BBO) as the quadratic medium. At wavelengths provided by standard laser sources, experimental conditions with both negligible GVD and significant GVM are not available, but the GVM (~ 200 fs/mm) and relatively high ratio of GVM to GVD at 800 nm allowed us to observe the steepening of 110-fs-wide initial Gaussian pulses after modest propagation lengths, ~ 1 cm. Thus, a Ti:sapphire regenerative amplifier operating at ≈ 800 nm wavelength was used as the source, which allows for suitable intensity at focus and a long enough confocal parameter to make the propagation effectively one dimensional. The high damage threshold of the BBO crystal is a crucial feature, as will be discussed below. Finally, its high d_{eff} and low n_2 make it possible to achieve $(n_2)_{\text{tot}}=0$.

We began by determining Δk_{ZSPM} . To do this, we used high incident pulse intensity and tuned the propagation direction away from the SHG phase-matching angle (in the direction appropriate for self-defocusing $\chi^{(2)}$ phase shifts), until we could see no change to the power spectrum, i.e., no SPM-induced spectral broadening. This was then repeated in several steps, increasing the intensity and retuning the angle. At high intensities the spectral shape is very sensitive to variations of Δk about Δk_{ZSPM} , with changes of only 0.1° (corresponding to ~ 1 π /mm) resulting in noticeable changes in the spectrum. We found $\Delta k_{\text{ZSPM}}=-31 \pm 5$ π /mm,

with the largest measurement error resulting from uncertainty in the SHG phase-matching angle. This implies $n_2 = (4.6 \pm 0.8) \times 10^{-16} \text{ cm}^2/\text{W}$ (assuming $d_{\text{eff}} = 1.8 \text{ pm}/\text{V}$), in line with accepted values [12]. With Δk_{ZSPM} and n_2 experimentally determined, the simulations suggested 8 mm to be a suitable propagation length, for which the maximum steepening occurs at intensity $\approx 0.7 \text{ TW}/\text{cm}^2$.

We measured the damage threshold for 110 fs pulses at $\Delta k_{\text{ZSPM}} = -31 \pi/\text{mm}$, and found it to be suitably high. For both coated and uncoated BBO crystals, damage to the input surface occurs before there is visible damage to the bulk, at intensities of 4.4 ± 1.0 and $4.0 \pm 0.9 \text{ TW}/\text{cm}^2$, respectively, which allowed us to aim for the optimum intensity of $0.7 \text{ TW}/\text{cm}^2$ without worrying about possible damage. The uncertainty in experimentally measured intensities was $\sim 20\%$. The $4 \text{ TW}/\text{cm}^2$ intensity might have damaged the BBO crystal if SPM-induced self-focusing had been present: $n_2 = 4.6 \times 10^{-16} \text{ cm}^2/\text{W}$ implies that a nonlinear phase of 1.0 rad is accumulated by a $1.0 \text{ TW}/\text{cm}^2$ pulse in only $280 \mu\text{m}$ of propagation. This would cause self-focusing collapse of a $100\text{-}\mu\text{m}$ -radius focused beam after propagating $\sim 6 \text{ mm}$. However, with the self-focusing suppressed, there is no possibility of damage due to collapse.

At incident intensities of $\geq 0.4 \text{ TW}/\text{cm}^2$, we observed bright color generation in cones about the propagation axis in the 8-mm-long crystal, which restricted our experiments to intensities $\leq 1.0 \text{ TW}/\text{cm}^2$. The observed colors cover the visible spectrum and form an emission pattern more complex than the previously observed concentric colored conical emission pattern at SHG phase matching [13]. At $1.0 \text{ TW}/\text{cm}^2$, there is already a few percent conversion of the FF energy to off-axis emission. As intensity increases, the conversion increases steadily to over 50%, producing a complex pattern of bright white light in a cone about the beam center, before the surface damage finally occurs at $4 \text{ TW}/\text{cm}^2$. The enhancement of the conversion with the increase of the intensity and propagation distance are signatures of modulation instability. These instabilities amplify fluctuations of the initial FF power, which hamper systematic measurements above $1.0 \text{ TW}/\text{cm}^2$. Above this intensity, the loss to the conical emission may become a significant effect as well. We note that the two-photon absorption edge in BBO is below 400 nm [15], which allowed us to ignore this loss channel.

The experimental setup was as follows. The 110 fs, 1 mJ pulse from the regenerative amplifier was split, with one half focused in an 8-mm-long BBO crystal oriented such that $\Delta k = -31 \pi/\text{mm}$, and the other half sent to a 25 mm BBO crystal to compress the pulse to 50 fs, using the $\chi^{(2)}:\chi^{(2)}$ soliton-compression technique [14]. The 50 fs pulse was used as a reference pulse for cross-correlation (CC) measurements of the steepened signal. In the absence of the 8 mm BBO crystal, the focused beam, with $120 \mu\text{m}$ radius and pulse energy up to $50 \mu\text{J}$ ($1.0 \text{ TW}/\text{cm}^2$ intensity), does not feature spectral modulation due to nonlinear phase accumulation in air. The centers of the experimental beam and 50 fs reference beam were recombined with a variable path-length delay in a $100\text{-}\mu\text{m}$ -thick BBO sample to produce the CC by SHG. Auto- and cross-correlation measurements of the input pulse were consistent.

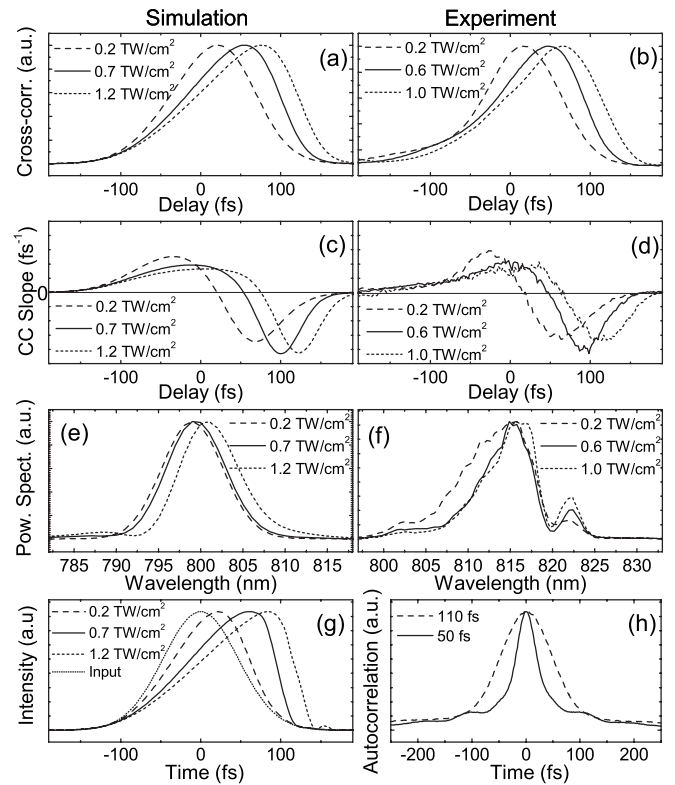


FIG. 2. Cross-correlations as predicted by the simulations (a) versus experimentally observed cross-correlations (b) for 110 fs Gaussian pulses after passing 8 mm in BBO at $\Delta k = -31 \pi/\text{mm}$ and at various intensities. (c), (d) The first derivative of (a) and (b), respectively. (e), (f) Spectra; (g) simulated temporal profiles that were used to generate (a). (h) The experimental autocorrelations of the input pulse and 50 fs cross-correlation reference pulse.

At intensities up to $1.0 \text{ TW}/\text{cm}^2$ we observe the steepening predicted by both the CLLE and the full equations (3). The measured CC traces at selected intensities are shown in Fig. 2(b), along with simulated CCs generated by Eqs. (3) with identical parameters [see Fig. 2(a)]; the intensities differ slightly, and were chosen to match the experimental data. Both the CCs and their temporal derivatives, Fig. 2(d), closely match the numerical results. We note that the experimental data also match well with simulations of Eq. (5): differences in the solutions of Eqs. (3) and (5) are of minor detail. At $0.2 \text{ TW}/\text{cm}^2$, there is very slight pulse tilting. At $0.6 \text{ TW}/\text{cm}^2$, there is significant steepening of the trailing edge and softening of the leading edge. Finally, at $1.0 \text{ TW}/\text{cm}^2$ the trailing edge is less steep. The CC has a smoothing effect on the pulse shape: the intensity profiles used to generate Fig. 2(a) exhibit clearer steepening [see Fig. 2(g)]. The experimental spectra also closely match spectra predicted by simulation of Eqs. (3) [see Figs. 2(e) and 2(f)], and, as predicted by the CLLE, the spectral broadening (on the linear scale) is negligible. The slight difference in spectral shapes between Figs. 2(e) and 2(f) may be attributed to details of the input experimental spectrum. Both the simulations and experiments show an unexpected slight redshift at the highest intensity. The simulations of both Eqs. (3) and Eq. (5) included third-order dispersion, which, however, produced an insignificant effect.

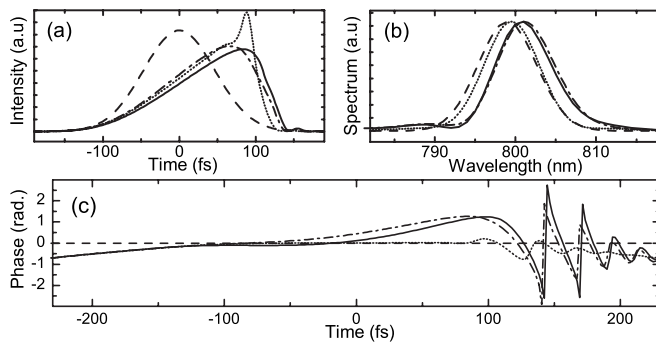


FIG. 3. Simulations corresponding to the case of 1.2 TW/cm^2 intensity in Fig. 2, using the coupled two-field equations, Eq. (3) (solid line), CLLE, Eq. (5) (dotted line), and the CLLE with the extra quintic term, $i|a|^4a$ (dash-dotted line). Dashed line is input. (a) Temporal profiles, (b) power spectra, and (c) temporal phase profiles.

The measured pulses agree well with the numerical predictions of Eqs. (3), and both confirm the character of the evolution expected from the CLLE, viz., temporal steepening without substantial spectral broadening. We also notice slight discrepancies at 1.0 TW/cm^2 : the redshift of the spectrum and slight increase in the temporal width of the pulse, observed in this case, cannot be explained by the CLLE. The decrease in steepening observed at 1.0 TW/cm^2 is not predicted either, as the steepening should increase monotonically. These discrepancies are consequences of using the high intensity necessary for our experiment in BBO at 800 nm wavelength. Despite the nominal cancellation of the $\chi^{(3)}$ and cascaded $\chi^{(2)}$ phase shifts, the simulated temporal phase profiles feature a SPM-like modulation that becomes significant at 1.0 TW/cm^2 (see solid line in Fig. 3). Further analysis of these phase shifts reveals that they grow in proportion to the squared intensity, which suggests the presence of an effective $\chi^{(5)}$ term as a higher-order perturbation to the effective CLLE, Eq. (5).

Indeed, an effective quintic term has been derived previously as a correction to the cascading-limit approximation [16], and it must appear as well in the perturbation expansion which was used to reduce Eqs. (3) to the single-field equation, Eq. (4) [note that direct $\chi^{(5)}$ effects are not included in the underlying model based on Eqs. (3)]. This correction should be significant only at extreme intensities, and has not been identified in previous experimental work, likely due to the (usual) domination of cubic SPM. A positive phase shift from the effective quintic term thus derived can explain both the temporal broadening (positive phase shifts and simultaneous action of normal GVD stretch the pulse) and redshift (an intensity-dependent phase shift applied to an asymmetric pulse results in a spectral shift [2]). These distortions, in turn, explain the decrease in pulse steepness observed at 1.0 TW/cm^2 . Figure 3 displays results corresponding to the 1.2 TW/cm^2 case of Fig. 2, obtained from simulations of the two-field equations (3), the CLLE (5), and the CLLE with an added $i|a|^4a$ term. The match between the results produced by Eqs. (3) and the $\chi^{(5)}$ -perturbed CLLE for the 1.2 TW/cm^2 intensity indicate a deviation from the CLLE model in the limit of extremely high intensities. In practice, this regime can be avoided by properly choosing experimental parameters, e.g., selecting larger GVM and thus stronger self-steepening. We note that the quintic term produces negligible effects at 0.2 and 0.6 TW/cm^2 , so the CLLE model is adequate for intensities up to 0.6 TW/cm^2 [simulations of Eqs. (3) and (5) match].

In conclusion, we have demonstrated clear theoretical and experimental evidence of an alternative governing equation in nonlinear optical pulse propagation, the Chen-Lee-Liu equation. The ability to shape pulses through self-steepening in the absence of SPM may find straightforward applications in studies of light-matter interactions.

This work was supported by NSF Grant Nos. PHY-0099564 and ECS-0217958. The authors thank Franz Kärtner for a helpful discussion.

-
- [1] T. Brabec and F. Krausz, *Phys. Rev. Lett.* **78**, 3282 (1997).
 [2] D. Anderson and M. Lisak, *Phys. Rev. A* **27**, 1393 (1983); G. Yang and Y. R. Shen, *Opt. Lett.* **9**, 510 (1984).
 [3] D. J. Kaup and A. C. Newell, *J. Math. Phys.* **19**, 798 (1978).
 [4] H. H. Chen, Y. C. Lee, and C. S. Liu, *Phys. Scr.* **20**, 490 (1979).
 [5] F. Verheest and B. Buti, *J. Plasma Phys.* **47**, 15 (1992).
 [6] G. Stegeman *et al.*, *Novel Optical Materials and Applications* (John Wiley & Sons, New York, 1997), pp. 49–76.
 [7] F. Wise, L. Qian, and X. Liu, *J. Nonlinear Opt. Phys. Mater.* **11**, 317 (2002).
 [8] R. DeSalvo *et al.*, *Opt. Lett.* **17**, 28 (1992).
 [9] F. Ö. Ilday *et al.*, *J. Opt. Soc. Am. B* **21**, 376 (2004).
 [10] J. Moses and F. W. Wise, *Phys. Rev. Lett.* **97**, 073903 (2006).
 [11] S. Kakei, N. Sasa, and J. Satsuma, *J. Phys. Soc. Jpn.* **64**, 1519 (1995); K. Kondo, K. Kajiwara, and K. Matsui, *ibid.* **66**, 60 (1997).
 [12] M. Sheik-Bahae and M. Ebrahimzadeh, *Opt. Commun.* **142**, 294 (1997); F. Hache, A. Zeboulon, G. Gallot, and G. M. Gale, *Opt. Lett.* **20**, 1556 (1995).
 [13] H. Zeng, J. Wu, H. Xu, K. Wu, and E. Wu, *Phys. Rev. Lett.* **92**, 143903 (2004); S. Trillo *et al.*, *Opt. Lett.* **27**, 1451 (2002).
 [14] S. Ashihara, J. Nishina, T. Shimura, and K. Kuroda, *J. Opt. Soc. Am. B* **19**, 2505 (2002); see also J. Moses and F. W. Wise, *Opt. Lett.* **31**, 1881 (2006); X. Liu, L. Qian, and F. W. Wise, *ibid.* **24**, 1777 (1999).
 [15] R. DeSalvo *et al.*, *IEEE J. Quantum Electron.* **32**, 1324 (1996).
 [16] J. P. Torres and L. Torner, *Opt. Quantum Electron.* **29**, 757 (1997).